

1 Interaction of CO₂ concentrations and water stress in 2 semi-arid plants causes diverging response in instantaneous 3 water use efficiency and carbon isotope composition

4 Na Zhao^{1,3}, Ping Meng², Yabing He¹, Xinxiao Yu^{1,3*}

5 ¹ College of soil and water conservation, Beijing Forestry University, Beijing 100083, P.R. China

6 ² Research Institute of Forestry, Chinese Academy of Forestry 100091, Beijing, P.R. China

7 ³ Beijing collaborative innovation center for eco-environmental improvement with forestry and
8 fruit trees

9 **Abstract.** In the context of global warming attributable to the increasing levels of CO₂, severe drought
10 may be more frequent in areas with chronic water shortages (semi-arid areas). This necessitates
11 on the interactions between increased levels of CO₂ and drought on plant photosynthesis. It is
12 reported that ¹³C fractionation occurs as CO₂-gas diffuses from the atmosphere to the sub-stomatal
13 Few researchers have investigated ¹³C fractionation at the site of carboxylation to cytoplasm before
14 sugars are exported outward from the leaf. This process typically progresses in response to variations in
15 environmental conditions (i.e., CO₂ concentrations and water stress), including in their interaction.
16 Therefore, saplings of two typical plant species (*Platycladus orientalis* and *Quercus variabilis*) from
17 semi-arid areas of Northern China were selected and cultivated in growth chambers with orthogonal
18 treatments (four CO₂ concentration ([CO₂]) × five soil volumetric water content (SWC)). The δ¹³C of
19 water-soluble compounds extracted from leaves of saplings was determined for an assessment of
20 instantaneous water use efficiency (WUE_{cp}) after cultivation. Instantaneous water use efficiency
21 derived from gas-exchange measurements (WUE_{ge}) was integrated to estimate differences in δ¹³C
22 signal variation before leaf-level translocation of primary assimilates. The WUE_{ge} in *P. orientalis* and
23 *Q. variabilis* both decreased with increased soil moisture at 35–80% of field capacity (FC), and
24 increased with elevated [CO₂] by increasing photosynthetic capacity and reducing transpiration.
25 Instantaneous water use efficiency (iWUE) according to environmental changes, differed between the
26 two species. The WUE_{ge} in *P. orientalis* was significantly greater than that in *Q. variabilis*, while an
27 opposite tendency was observed when comparing WUE_{cp} between the two species. Total ¹³C
28 fractionation at the site of carboxylation to cytoplasm before sugar export (total ¹³C fractionation) was
29 species-specific, as demonstrated in the interaction of [CO₂] and SWC. Rising [CO₂] coupled with
30 moistened soil generated increasing disparities in δ¹³C between water-soluble compounds (δ¹³C_{WSC})
31 and estimates based on gas-exchange observations (δ¹³C_{obs}) in *P. orientalis*, ranging between 0.0328–
32 0.0472‰. Differences between δ¹³C_{WSC} and δ¹³C_{obs} in *Q. variabilis* increased as [CO₂] and SWC
33 increased (0.0384–0.0466‰). The ¹³C fractionation from mesophyll conductance (*g_m*) and
34 post-carboxylation both contributed to the total ¹³C fractionation that was determined by δ¹³C of
35 water-soluble compounds and gas-exchange measurements. Total ¹³C fractionation was linearly
36 dependent on stomatal conductance, indicating post-carboxylation fractionation could be attributed to
37 environmental variation. The magnitude and environmental dependence of apparent post-carboxylation
38 fractionation is worth our attention when addressing photosynthetic fractionation.

39 **Key words:** Post-carboxylation fractionation; Carbon isotope fractionation; Elevated CO₂
40 concentration; Soil volumetric water content; Instantaneous water use efficiency

41 **1 Introduction**

42 Since the industrial revolution, atmospheric CO₂ concentration has increased at an annual rate of
43 0.4%, and is expected to increase to 700 μmol·mol⁻¹, culminating in more frequent periods of dryness
44 (IPCC, 2014). Increasing atmospheric CO₂ concentrations that exacerbate the greenhouse effect will
45 increase fluctuations in global precipitation patterns, which will probably amplify drought frequency in
46 arid regions and lead to more frequent extreme flooding events in humid regions (Lobell et al., 2014).
47 Accompanying the increasing concentration of CO₂, mean δ¹³C of atmospheric CO₂ is currently being
48 depleted by 0.02–0.03‰ year⁻¹ (CU-INSTAAR/NOAACMDL network for atmospheric CO₂;
49 <http://www.esrl.noaa.gov/gmd/>).

50 The current carbon isotopic composition may respond to environmental change and its influence on
51 diffusion via plant physiological and metabolic processes (Gessler et al., 2014; Streit et al., 2013).
52 While depletion of δ¹³C_{CO₂} is occurring in the atmosphere, variations in CO₂ concentration ([CO₂])
53 may affect δ¹³C of plant organs which, in turn, respond physiologically to changes in climate (Gessler
54 et al., 2014). The carbon discrimination (¹³Δ) in leaves could also provide timely feedback to the
55 availability of soil moisture and atmospheric vapor pressure deficit (Cernusak et al., 2012).
56 Discrimination of ¹³C in leaves relies mainly on environmental factors that affect the ratio of
57 intercellular to ambient [CO₂] (C_i/C_a). Rubisco activities and the mesophyll conductance derived from
58 the difference of [CO₂]s between intercellular sites and chloroplasts are also involved (Farquhar et al.,
59 1982; Cano et al., 2014). Changes in environmental conditions affect photosynthetic discrimination,
60 recording differentially in the δ¹³C of water-soluble compounds (δ¹³C_{WSC}) in different plant organs.
61 Several processes during photosynthesis alter the δ¹³C of carbon transported within plants.
62 Carbon-fractionation during photosynthetic CO₂ fixation has been reviewed elsewhere (Farquhar et al.,
63 1982; Farquhar and Sharkey, 1982).

64 Post-photosynthetic fractionation is derived from equilibrium and kinetic isotopic effects that
65 determine isotopic differences between metabolites and intramolecular reaction positions. These are
66 defined as “post-photosynthetic” or “post-carboxylation” fractionation (Jäggi et al., 2002; Badeck et al.,
67 2005; Gessler et al., 2008). Post-carboxylation fractionation in plants includes the carbon
68 discrimination that follows carboxylation of **ribulose-1, 5-bisphosphate and internal diffusion** (RuBP,
69 27‰), as well as related transitory starch metabolism (Gessler et al., 2008; Gessler et al., 2014),
70 fractionation-associated phloem transport, remobilization or storage of soluble carbohydrates, and
71 starch metabolism fractionation in sink tissue (tree rings). In the synthesis of soluble sugars,
72 ¹³C-depletions of triose phosphates occur during export from the cytoplasm, and during production of
73 fructose-1, 6-bisphosphate by aldolase in transitory starch synthesis (Rossmann et al., 1991;
74 Gleixner and Schmidt, 1997). Synthesis of sugars before transportation to the twig is associated with
75 the post-carboxylation fractionation generated in leaves. Although these are likely to play a role,
76 another consideration is [CO₂] in the chloroplast (C_c), not in the intercellular space, as considered in the
77 simplified equation of Farquhar’s model (Evans et al., 1986; Farquhar et al., 1989) is actually defined
78 as carbon isotope discrimination (δ¹³C). Differences between gas-exchange derived values and online
79 measurements of δ¹³C have often been used to estimate C_i-C_c and mesophyll conductance for CO₂ (Le
80 Roux et al., 2001; Warren and Adams, 2006; Flexas et al., 2006; Evans et al., 2009; Flexas et al., 2012;
81 Evans and von Caemmerer 2013). In this regard, changes in mesophyll conductance could be partly

82 responsible for the differences in the two measurements, as it generally increases in the short term in
83 response to elevated CO₂ (Flexas et al., 2014), but tends to decrease under drought (Hommel et al.,
84 2014; Théroux-Rancourt et al., 2014). Therefore, it is necessary to avoid confusion between carbon
85 isotope discrimination derived from synthesis of soluble sugars and/or mesophyll conductance. The
86 degree to which carbon fractionation is related to environmental variation has yet to be fully
87 investigated.

88 The simultaneous isotopic analysis of leaves allows determination of temporal variation in isotopic
89 fractionation (Rinne et al., 2016). This will aid in an accurate recording of environmental conditions.
90 Newly assimilated carbohydrates can be extracted, and these are termed the water-soluble compounds
91 (WSCs) in leaves (Brandes et al., 2006; Gessler et al., 2009). WSCs can also be associated with an
92 assimilation-weighted mean of C_i/C_a (and C_c/C_a) photosynthesized over periods ranging from a few
93 hours to 1–2 days (Pons et al., 2009). However, there is disagreement whether fractionation caused by
94 post-carboxylation and/or mesophyll resistance can alter the stable signatures of leaf carbon and thence
95 influence instantaneous water use efficiency (iWUE). In addition, the manner in which iWUE derived
96 from isotopic fractionation responds to environmental factors, such as elevated [CO₂] and/or soil water
97 gradients, is largely unknown.

98 Consequently, we investigated the $\delta^{13}\text{C}$ of the fast-turnover carbohydrate pool in sapling leaves of
99 two tree species, *Platycladus orientalis* (L.) Franco and *Quercus variabilis* Bl., native to semi-arid
100 areas of China. We conducted gas-exchange measurements in controlled-environment growth
101 chambers. One goal is to differentiate the ^{13}C fractionation from the site of carboxylation to cytoplasm
102 prior to sugar transportation in *P. orientalis* and *Q. variabilis*, which is the total ^{13}C fractionation
103 determined from the $\delta^{13}\text{C}$ of WSCs and gas-exchange measurements. Another goal is to discuss the
104 potential causes for the observed divergence, estimate contributions of post-photosynthesis and
105 mesophyll conductance on these differences, and describe how carbon isotopic fractionation responds
106 to the interactive effects of elevated [CO₂] and water stress.

107 2 Material and Methods

108 2.1 Study site and design

109 *P. orientalis* and *Q. variabilis* saplings, selected as experimental material, were obtained from the
110 Capital Circle forest ecosystem station, a part of the Chinese Forest Ecosystem Research Network
111 (CFERN), 40°03'45"N, 116°5'45"E, Beijing, China. This region is forested by *P. orientalis* and *Q.*
112 *variabilis*. We chose saplings of similar basal diameters, heights, and growth class. Each sapling was
113 placed into an individual pot (22 cm diam. × 22 cm high). Undisturbed soil samples were collected
114 from the field, sieved (with particles >10 mm removed), and placed into the pots. The soil bulk density
115 in the pots was maintained at 1.337–1.447 g cm⁻³. After a 30-day transplant recovery period, the
116 saplings were placed into growth chambers for orthogonal cultivation.

117 The controlled experiment was conducted in growth chambers (FH-230, Taiwan Hipoint
118 Corporation, Kaohsiung City, Taiwan). To reproduce the meteorological conditions of different
119 growing seasons in the research region, daytime and nighttime temperatures in the chambers were set
120 to 25 ± 0.5°C from 07:00 to 17:00 and 18 ± 0.5°C from 17:00 to 07:00. Relative humidity was
121 maintained at 60% and 80% during the daytime and nighttime, respectively. The mean daytime light
122 intensity was 200–240 μmol m⁻² s⁻¹. The chamber system was designed to control and monitor [CO₂].
123 Two growth chambers (A and B) were used in this study. Chamber A maintained [CO₂] at 400 (C₄₀₀)

124 and 500 ppm (C_{500}). Chamber B maintained $[CO_2]$ at 600 (C_{600}) and 800 ppm (C_{800}). The target $[CO_2]$
125 in each chamber had a standard deviation of ± 50 ppm during plant cultivation and testing.

126 An automatic watering device was used to irrigate the potted saplings to avoid heterogeneity when
127 scheduled watering was not made (Fig. 1). The watering device consisted of a water storage tank,
128 holder, controller, soil moisture sensors, and a drip irrigation component. Prior to use, the tank was
129 filled with water, and the soil moisture sensor was inserted to a uniform depth in the soil. After
130 connecting the controller to an AC power supply, target soil volumetric water content (SWC) was set
131 and monitored by soil moisture sensors. Since changes in SWC could be sensed by the sensors, this
132 automatic watering device could be regulated to begin or stop watering the plants. One irrigation
133 device was installed per chamber. Based on mean field capacity (FC) of potted soil (30.70%), we
134 established orthogonal treatments of four $[CO_2] \times$ five SWC (Table. 1). In Table 1, A₁-A₄ denotes $[CO_2]$
135 of 400 (C_{400}), 500 (C_{500}), 600 (C_{600}) and 800 ppm (C_{800}) in the chambers; B₁-B₅ denotes 35–45%
136 (10.74–13.81%), 50–60% (15.35–18.42%), 60–70% (18.42–21.49%), 70–80% (21.49–24.56%), and
137 100% of FC (CK, 27.63–30.70%). Each orthogonal treatment of $[CO_2] \times$ SWC for two saplings per
138 species was repeated twice. Each treatment lasted 7 days. One pot was exposed in each of the $[CO_2] \times$
139 SWC treatments. Pots in the chambers were rearranged every two days to promote uniform
140 illumination.

141 2.2 Foliar gas exchange measurement

142 Fully expanded primary annual leaves of the saplings were measured with a portable infrared gas
143 photosynthesis system (LI-6400, Li-Cor, Lincoln, US) before and after the 7-day cultivation. Two
144 saplings per species were replicated per treatment (SWC \times $[CO_2]$). For each sapling, four leaves were
145 sampled and four measurements were conducted on each leaf. Main photosynthetic parameters, such as
146 net photosynthetic rate (P_n) and transpiration rate (T_r), were measured. Based on theoretical
147 considerations of Von Caemmerer and Farquhar (1981), stomatal conductance (g_s) and intercellular
148 $[CO_2]$ (C_i) were calculated by the Li-Cor software. Instantaneous water use efficiency via gas exchange
149 (WUE_{ge}) was calculated as the ratio P_n / T_r .

150 2.3 Plant material collection and leaf water-soluble compounds extraction

151 Eight recently-expanded sun leaves were selected per sapling and homogenized in liquid nitrogen
152 after gas-exchange measurements were finished. For extraction of WSCs from the leaves (Gessler et al.,
153 2004), 50 mg of grounded leaves and 100 mg of PVPP (polyvinylpyrrolidone) were mixed and
154 incubated in 1 mL distilled water for 60 min at 5°C in a centrifuge tube. Each leaf sample was
155 replicated twice. The tubes containing the mixture were heated in 100°C water for 3 min. After cooling
156 to room temperature, the supernatant of the mixture was centrifuged (12000 $\times g$ for 5 min) and 10 μ L
157 of supernatant was transferred into a tin capsule and dried at 70°C. Folded capsules were used for $\delta^{13}C$
158 analysis of WSCs. The samples of WSCs from leaves were combusted in an elemental analyzer
159 (EuroEA, HEKAtech GmbH, Wegberg, Germany) and analyzed with a mass-spectrometer
160 (DELTA^{plus}XP, ThermoFinnigan).

161 Carbon isotope signatures were expressed in δ -notation (parts per thousand), relative to the
162 international Pee Dee Belemnite (PDB) standard:

$$163 \delta^{13}C = \left(\frac{R_{sample}}{R_{standard}} - 1 \right) \times 1000 \quad (1)$$

164 where $\delta^{13}C$ is the heavy isotope and R_{sample} and $R_{standard}$ refer to the isotope ratio between the particular
165 substance and the corresponding standard, respectively. The precision of repeated measurements was

166 0.1 ‰.

167 2.4 Isotopic calculation

168 2.4.1 ¹³C fractionation from the site of carboxylation to cytoplasm prior to sugar transportation

169 Based on the linear model of Farquhar and Sharkey (1982), the isotope discrimination, Δ , was
170 calculated as

$$171 \Delta = (\delta^{13}C_a - \delta^{13}C_{WSC}) / (1 + \delta^{13}C_{WSC}), \quad (2)$$

172 where $\delta^{13}C_a$ and $\delta^{13}C_{WSC}$ are the isotope signatures of ambient [CO₂] in chambers and WSCs extracted
173 from leaves, respectively. The $C_i:C_a$ was determined by

$$174 C_i:C_a = (\Delta - a) / (b - a), \quad (3)$$

175 where C_i and C_a are the [CO₂] within substomatal cavities and in growth chambers, respectively; a is
176 the fractionation occurring CO₂ diffusion in still air (4‰) and b refers to the discrimination during CO₂
177 fixation by ribulose 1,5- biphosphate carboxylase/oxygenase (Rubisco) and internal diffusion (30‰).
178 Instantaneous water use efficiency by gas-exchange measurement (WUE_{ge}) was calculated as

$$179 WUE_{ge} = P_n : T_r = (C_a - C_i) / 1.6\Delta e, \quad (4)$$

180 where 1.6 is the diffusion ratio of stomatal conductance for water vapor to CO₂ in chambers and Δe is
181 the difference between e_{lf} and e_{atm} , representing the extra- and intra-cellular water vapor pressure,
182 respectively:

$$183 \Delta e = e_{lf} - e_{atm} = 0.611 \times e^{17.502T / (240.97 + T)} \times (1 - RH), \quad (5)$$

184 where T and RH are the leaf-surface temperature and relative humidity, respectively. Combining Eqns.
185 (2, 3 and 4), the instantaneous water use efficiency was determined by the $\delta^{13}C_{WSC}$ of leaves, defined
186 as:

$$187 WUE_{cp} = \frac{P_n}{T_r} = (1 - \varphi) (C_a - C_i) / 1.6\Delta e = C_a (1 - \varphi) \left[\frac{b - \delta^{13}C_a + (b+1)\delta^{13}C_{WSC}}{(b-a)(1 + \delta^{13}C_{WSC})} \right] / 1.6\Delta e, \quad (6)$$

188 where φ is the respiratory ratio of leaf carbohydrates to other organs at night (0.3).

189 Then the ¹³C fractionation from the site of carboxylation to cytoplasm prior to sugar transportation
190 (defined as the total ¹³C fractionation) was estimated by the observed $\delta^{13}C$ of WSCs from leaves
191 ($\delta^{13}C_{WSC}$) and the modeled $\delta^{13}C$ calculated from gas-exchange measurements ($\delta^{13}C_{model}$). The $\delta^{13}C_{model}$
192 was calculated by Δ_{model} from Eqn. (2); Δ_{model} was determined by combining Eqns. (3 and 4) as

$$193 \Delta_{model} = (b - a) \left(1 - \frac{1.6\Delta e WUE_{ge}}{C_a} \right) + a, \quad (7)$$

$$194 \delta^{13}C_{model} = \frac{C_a - \Delta_{model}}{1 + \Delta_{model}}, \quad (8)$$

$$195 \text{Total } ^{13}\text{C fractionation} = \delta^{13}C_{WSC} - \delta^{13}C_{model}. \quad (9)$$

196 2.4.2 Method of estimating mesophyll conductance and the contribution of post-carboxylation 197 fractionation

198 CO₂ diffusion into photosynthetic sites includes two main processes. CO₂ **firstly** moves from
199 ambient air surrounding the leaf (C_a) through stomata to the sub-stomatic cavities (C_i). From
200 sub-stomatic **cavities**, CO₂ then moves to the sites of carboxylation within the chloroplast stroma (C_c)

201 of the leaf mesophyll. The latter procedure of diffusion is termed mesophyll conductance (g_m ; Flexas et al., 2008). The carbon isotope discrimination was generated from the relative contribution of diffusion
 202 and carboxylation, reflected by C_c to C_a . The carbon isotopic discrimination (Δ) can be presented as
 203 (Farquhar et al. 1982):
 204

$$205 \quad \Delta = a_b \frac{C_a - C_s}{C_a} + a \frac{C_s - C_i}{C_a} + (e_s + a_l) \frac{C_i - C_c}{C_a} + b \frac{C_c}{C_a} - \frac{eR_D + f\Gamma^*}{C_a}, \quad (10)$$

206 where C_a , C_s , C_i , and C_c are the $[\text{CO}_2]$ in the ambient air, at the boundary layer of the leaf, in the
 207 substomatal cavities, and at the sites of carboxylation, respectively; a_b is the CO_2 diffusional
 208 fractionation at the boundary layer (2.9‰); e_s is the discrimination for CO_2 diffusion when CO_2 enters
 209 in solution (1.1‰, at 25°C); a_l is the CO_2 diffusional fractionation in the liquid phase (0.7‰); e and f
 210 are carbon discriminations derived in dark respiration (R_D) and photorespiration, respectively; k is the
 211 carboxylation efficiency, and Γ^* is the CO_2 compensation point in the absence of dark respiration
 212 (Brooks and Farquhar, 1985).

213 When gas in the cuvette is well stirred during gas-exchange measurements, diffusion across the
 214 boundary layer is negligible and Eqn. (10) can be written as

$$215 \quad \Delta = a \frac{C_a - C_i}{C_a} + (e_s + a_l) \frac{C_i - C_c}{C_a} + b \frac{C_c}{C_a} - \frac{eR_D + f\Gamma^*}{C_a}. \quad (11)$$

216 There is no consensus about the value of e , although recent measurements estimate it as ranging
 217 from 0-4‰. The value of f has been estimated to range from 8-12‰ (Gillon and Griffiths, 1997;
 218 Igamberdiev et al., 2004; Lanigan et al., 2008). As the most direct factor, b influences the calculation of
 219 g_m , which is thought to be approximately 30‰ in higher plants (Guy et al., 1993).

220 The difference of $[\text{CO}_2]$ between substomatal cavities and chloroplasts is omitted, while diffusion
 221 related to dark-respiration and photorespiration are negligible and Eqn. (11) may be simplified to

$$222 \quad \Delta_i = a + (b - a) \frac{C_i}{C_a}. \quad (12)$$

223 Eqn. (12) denotes the linear relationship between carbon discrimination and C_i/C_a . This underlines
 224 subsequent comparison between expected Δ (originating from gas-exchange, Δ_i , and measured Δ_{obs}),
 225 which can be used to evaluate the differences of $[\text{CO}_2]$ between intercellular air and sites of
 226 carboxylation associated with ^{13}C fractionation from mesophyll conductance. Consequently, g_m is
 227 calculated by subtracting the Δ_{obs} of Eqn. (11) from Δ_i [Eqn. (12)]:

$$228 \quad \Delta_i - \Delta_{obs} = (b - e_s - a_l) \frac{C_i - C_c}{C_a} + \frac{eR_D + f\Gamma^*}{C_a} \quad (13)$$

229 and P_n from Fick's first law relates

$$230 \quad P_n = g_m (C_i - C_c). \quad (14)$$

231 Substituting Eqn. (14) into Eqn. (13) gives us

$$232 \quad \Delta_i - \Delta_{obs} = (b - e_s - a_l) \frac{P_n}{g_m C_a} + \frac{eR_D + f\Gamma^*}{C_a}, \text{ and} \quad (15)$$

$$233 \quad g_m = \frac{(b - e_s - a_l) \frac{P_n}{C_a}}{(\Delta_i - \Delta_{obs}) - \frac{eR_D + f\Gamma^*}{C_a}}. \quad (16)$$

234 In the calculation of g_m , terms of **respiration and photorespiration can** be ignored and e and f are
235 assumed to be zero or cancelled in the calculation of g_m .

236 Then Eqn. (16) can be rewritten as

$$237 \quad g_m = \frac{(b-e_s-a_l)\frac{P_n}{C_a}}{\Delta_i-\Delta_{obs}}. \quad (17)$$

238 Therefore, the contribution of post-carboxylation fractionation can be estimated by

$$239 \quad \text{Contribution of post-carboxylation fractionation} = \frac{(\text{Total } ^{13}\text{C fractionation} - \text{fractionation from mesophyll conductance})}{\text{Total } ^{13}\text{C fractionation}} \times 100\%. \quad (18)$$

241 **3 Results**

242 **3.1 Foliar gas exchange measurements**

243 When SWC increased between the treatments, P_n , g_s and T_r in *P. orientalis* and *Q. variabilis* peaked
244 at 70–80% of FC **and** 100% of FC (Fig. 2). The C_i in *P. orientalis* rose as SWC increased. It peaked at
245 60–70% of FC and declined thereafter with increased SWC in *Q. variabilis*. The carbon uptake and C_i
246 were significantly improved by elevated $[\text{CO}_2]$ at all SWC for the two species ($p < 0.05$). Greater
247 increases **in** P_n in *P. orientalis* were found at 50–70% of FC from C_{400} to C_{800} , which was at 35–45% of
248 FC in *Q. variabilis*. As water stress was reduced (at 70–80% and 100% of FC), reduction of g_s in *P.*
249 *orientalis* was more pronounced with elevated $[\text{CO}_2]$ at a given SWC ($p < 0.01$). Nevertheless, g_s in *Q.*
250 *variabilis* for C_{400} , C_{500} , and C_{600} was significantly higher than that for C_{800} at 50–80% of FC ($p < 0.01$).
251 Coordinated with g_s , T_r of the two species for C_{400} and C_{500} was significantly higher than that for C_{600}
252 and C_{800} , except at 35–60% of FC ($p < 0.01$, Figs. 2g and 2h). P_n , g_s , C_i and T_r in *Q. variabilis* was
253 significantly greater than the corresponding values in *P. orientalis* ($p < 0.01$, Fig. 2).

254 **3.2 $\delta^{13}\text{C}$ of water-soluble compounds in leaves**

255 After observations of photosynthetic traits in leaves of the two species, the same leaves were
256 immediately frozen and WSCs were extracted for all orthogonal treatments. The carbon isotope
257 composition of WSCs ($\delta^{13}\text{C}_{\text{WSC}}$) of both species increased as SWC increased (Figs. 3a and 3b, $p < 0.01$).
258 The mean $\delta^{13}\text{C}_{\text{WSC}}$ of *P. orientalis* and *Q. variabilis* ranged from $-27.44 \pm 0.155\%$ to $-26.71 \pm 0.133\%$,
259 and from $-27.96 \pm 0.129\%$ to $-26.49 \pm 0.236\%$, respectively. The photosynthetic capacity varied with
260 increased SWC and the mean $\delta^{13}\text{C}_{\text{WSC}}$ of the two species, reaching their respective maxima at 70–80%
261 of FC. With gradual enrichment of $[\text{CO}_2]$, mean $\delta^{13}\text{C}_{\text{WSC}}$ in both species declined when $[\text{CO}_2]$ exceeded
262 600 ppm ($p < 0.01$). Except for C_{400} at 50–100% of FC, the $\delta^{13}\text{C}_{\text{WSC}}$ in *P. orientalis* was significantly
263 higher than that in *Q. variabilis* for most $[\text{CO}_2] \times \text{SWC}$ treatments ($p < 0.01$, Fig. 3).

264 **3.3 Estimations of WUE_{ge} and WUE_{cp}**

265 Figure 4a shows that increments of WUE_{ge} in *P. orientalis* under severe drought (i.e., 35–45% of FC)
266 were highest for most $[\text{CO}_2]$, ranging from **90.7 to 564.7%**. The WUE_{ge} in *P. orientalis* decreased as
267 SWC increased and increased as $[\text{CO}_2]$ elevated. Differing from variation in WUE_{ge} in *P. orientalis*
268 with moistened soil, WUE_{ge} in *Q. variabilis* increased slightly at 100% of FC for C_{600} or C_{800} (Fig. 4b).
269 The maximum WUE_{ge} occurred at 35–45% of FC for C_{800} among all orthogonal treatments associated
270 with both species. Elevated $[\text{CO}_2]$ enhanced the WUE_{ge} in *Q. variabilis* at **all** SWC, except at 60–80%
271 of FC. Thirty-two saplings of *P. orientalis* had greater WUE_{ge} than did *Q. variabilis* for the same $[\text{CO}_2]$

272 × SWC treatments ($p < 0.05$).

273 As illustrated in Fig. 5a, WUE_{cp} in *P. orientalis* for C_{600} or C_{800} increased as water stress was
274 alleviated beyond 50–60% of FC, as well as that for C_{400} or C_{500} , while SWC exceeded 60–70% of FC.
275 *Q. variabilis* showed variable WUE_{cp} with increasing SWC (Fig. 5b). Except for C_{400} , WUE_{cp} in *Q.*
276 *variabilis* decreased abruptly at 50–60% of FC, and then increased as SWC increased for C_{500} , C_{600} ,
277 and C_{800} . In contrast to the results for WUE_{ge} , WUE_{cp} in *Q. variabilis* was more pronounced than in *P.*
278 *orientalis* among all orthogonal treatments.

279 3.4 ^{13}C fractionation from the site of carboxylation to cytoplasm before sugar transportation

280 We evaluated the total ^{13}C fractionation from the site of carboxylation to the cytoplasm by
281 gas-exchange measurements and WSCs in leaves (Table 2), which can help track the path of ^{13}C
282 fractionation in leaves. Comparing $\delta^{13}C_{WSC}$ with $\delta^{13}C_{model}$ from Eqns. (4, 7–9), the total ^{13}C
283 fractionation in *P. orientalis* ranged from 0.0328 to 0.0472‰, which was less than that in *Q. variabilis*
284 (0.0384 to 0.0466‰). The total fractionation in *P. orientalis* was magnified with increasing SWC,
285 especially when SWC reached 35–80% of FC from C_{400} to C_{800} (increasing by 21.3–42.0%). The total
286 fractionation for C_{400} and C_{500} were amplified as SWC increased until 50–60% of FC in *Q. variabilis*,
287 whereas they were increased at 50–80% of FC and decreased at 100% of FC for C_{600} and C_{800} . Elevated
288 $[CO_2]$ enhanced the mean total fractionation in *P. orientalis*, while fractionation in *Q. variabilis*
289 declined sharply from C_{600} to C_{800} . Total ^{13}C fractionation in *P. orientalis*, with increased SWC,
290 increased more rapidly than it did in *Q. variabilis*.

291 3.5 g_m imposed on the interaction of CO_2 concentration and water stress

292 A comparison between online leaf $\delta^{13}C_{WSC}$ and the values desired from gas-exchange measurements
293 is given to estimate the g_m over all treatments in Fig. 6 [Eqns. (10–17)]. A significant increasing trend
294 occurred in g_m with decreasing water stress in *P. orientalis*, ranging from 0.0091–0.0690 mol CO_2
295 $m^{-2} s^{-1}$ ($p < 0.05$), reaching a maximum at 100% of FC under a given $[CO_2]$. Increases in g_m in *Q.*
296 *variabilis* with increasing SWC were not significant, except those under C_{400} . With increasing $[CO_2]$,
297 g_m in the two species increased at different rates. With *P. orientalis* under C_{400} , g_m increased gradually
298 and reached a maximum under C_{800} at 35–60% and 100% of FC ($p < 0.05$). However, that was
299 maximized under C_{600} ($p < 0.05$) and reduced under C_{800} at 60–80% of FC. The maximum increment in
300 g_m (8.2–58.4%) occurred at C_{800} at all SWC for *Q. variabilis*. The g_m in *Q. variabilis* was clearly
301 greater than that in *P. orientalis* under the same treatment conditions.

302 3.6 Contribution of post-carboxylation fractionation

303 We evaluated the difference between Δ_i and Δ_{obs} in ^{13}C fractionation derived from mesophyll
304 conductance. The post-photosynthetic fractionation after carboxylation can be calculated by subtracting
305 g_m -sourced fractionation from the total ^{13}C fractionation (Table 2). The g_m -sourced fractionation
306 provided a smaller contribution to the total ^{13}C fractionation than did post-carboxylation fractionation
307 irrespective of treatment (Table 2). The g_m -sourced fractionation in the two species illustrated different
308 variations with increasing SWC, which declined at 50–80% of FC and increased at 100% of FC in *P.*
309 *orientalis*; yet, in *Q. variabilis*, it increased with water stress alleviation at 50–80% of FC and then
310 decreased at 100% of FC. Nevertheless, in the two species post-carboxylation fractionation in leaves all
311 increased as SWC increased. The g_m -sourced fractionation in *P. orientalis* and *Q. variabilis* reached
312 their peaks under C_{600} and C_{800} , respectively. Post-carboxylation fractionation was magnified with
313 increases in $[CO_2]$ in *P. orientalis*, and reached a maximum under C_{600} and then declined under C_{800} .

314 3.7 Relationship between g_s , g_m and total ^{13}C fractionation

315 Total ^{13}C fractionation may be correlated with resistances associated with stomata and mesophyll
316 cells. We performed linear regressions between g_s/g_m and total ^{13}C fractionation in *P. orientalis* and *Q.*
317 *variabilis* (Fig. 7 and 8). The total ^{13}C fractionation was correlated to g_s ($p < 0.01$). The positive linear
318 relationships between g_m and total ^{13}C fractionation ($p < 0.01$) indicated that the variation of $[\text{CO}_2]$
319 through the chloroplast was correlated with carbon discrimination following leaf photosynthesis.

320 4 Discussion

321 4.1 Photosynthetic traits

322 The exchange of CO_2 and water vapor via stomata can be modulated by the soil/leaf water potential
323 (Robredo et al., 2010). Saplings of *P. orientalis* reached maximum P_n and g_s at 70–80% of FC
324 irrespective of $[\text{CO}_2]$ treatments. As SWC exceeded this soil water threshold, elevated CO_2 caused a
325 greater reduction in g_s as was previously reported for barley and wheat (Wall et al., 2011). The
326 decrease in g_s responding to elevated $[\text{CO}_2]$, could be mitigated with increases in SWC. The C_i in *Q.*
327 *variabilis* peaked at 60–70% of FC and then declined as soil moisture increased (Wall et al., 2006;
328 Wall et al., 2011). This may be because stomata tend to maintain a constant C_i or C_i/C_a when ambient
329 $[\text{CO}_2]$ is increased, which would determine the amount of CO_2 directly used in the chloroplast (Yu et
330 al., 2010). This result could be explained as stomatal limitation (Farquhar and Sharkey, 1982; Xu,
331 1997). However, C_i in *P. orientalis* increased considerably, while SWC exceeded 70–80% of FC, as
332 found by Mielke et al. (2000). One possible contributing factor is plants close their stomata to reduce
333 water loss during organic matter synthesis simultaneously decreasing the availability of CO_2 and
334 generating respiration of organic matter (Robredo et al., 2007). Another possible explanation is that the
335 limited root volume of potted plants may be unable to absorb sufficient water to support the full growth
336 of shoots (Leakey et al., 2009; Wall et al., 2011). In the present study, increasing $[\text{CO}_2]$ may cause
337 nonstomatal limitations when SWC exceeds a soil moisture threshold of 70–80% of FC. The
338 accumulation of nonstructural carbohydrates in leaf tissue may induce mesophyll-based and/or
339 biochemical-based transient inhibition of photosynthetic capacity (Farquhar and Sharkey, 1982). Xu
340 and Zhou (2011) developed a five-level SWC gradient to examine the effect of water on the physiology
341 of a perennial, *Leymus chinensis*, and demonstrated that there was a clear maximum in SWC, below
342 which the plant could adjust to changing environmental conditions. Micanda-Apodaca et al. (2014) also
343 concluded that in suitable water conditions, elevated CO_2 levels augmented CO_2 assimilation in
344 herbaceous plants.

345 The P_n of the two woody plant species increased with elevated $[\text{CO}_2]$ similar to results seen with
346 other C_3 woody plants (Kgope et al., 2010). Increasing $[\text{CO}_2]$ alleviated severe drought and the need for
347 heavy irrigation, suggesting that photosynthetic inhibition produced by a lack or excess of water may
348 be mediated by increased $[\text{CO}_2]$ (Robredo et al., 2007; Robredo et al., 2010) and ameliorate the effects
349 of drought stress by reducing plant transpiration (Kirkham, 2016; Kadam et al., 2014;
350 Micanda-Apodaca et al., 2014; Tausz-Posch et al., 2013).

351 4.2 Differences between WUE_{ge} and WUE_{cp}

352 Increases in WUE_{ge} in *P. orientalis* and *Q. variabilis* that resulted from the combination of P_n
353 increase and g_s decrease were followed by a reduction in T_r (Figs. 2a, 2g, 2b and 2h). This result was
354 also demonstrated by Ainsworth and McGrath (2010). Comparing P_n and T_r in the two species, a lower
355 WUE_{ge} in *Q. variabilis* was obtained due to its different physiological and morphological traits, such as
356 larger leaf area, rapid growth, and higher stomatal conductance than that in *P. orientalis* (Adiredjo et al.,

357 2014). Medlyn et al. (2001) reported that stomatal conductance of broadleaved species is more
358 sensitive to elevated $[\text{CO}_2]$ than conifer species. There is no agreement on the patterns of iWUE at the
359 leaf level, related to SWC (Yang et al., 2010). The WUE_{ge} in *P. orientalis* and *Q. variabilis* were
360 enhanced with soil drying, as presented by Parker and Pallardy (1991), DeLucia and Heckathorn
361 (1989), Reich et al. (1989), and Leakey (2009).

362 Bögelein et al. (2012) confirmed that WUE_{cp} was more consistent with daily mean WUE_{ge} than
363 with $\text{WUE}_{\text{phloem}}$ (calculated with the $\delta^{13}\text{C}$ of phloem). The WUE_{cp} of the two species demonstrated
364 similar variations to those in $\delta^{13}\text{C}_{\text{WSC}}$, which differed from those of WUE_{ge} . Pons et al. (2009) noted
365 that Δ of leaf soluble sugar is coupled with environmental dynamics over a period ranging from a few
366 hours to 1–2 days. The WUE_{cp} of our materials responded to $[\text{CO}_2] \times \text{SWC}$ treatments over a number
367 of **cultivation days**, whereas WUE_{ge} was characterized as the instantaneous physiological change in
368 plants to new conditions. Consequently, WUE_{cp} and WUE_{ge} had different degrees of **variation** in
369 response to different treatments.

370 **4.3 Influence of mesophyll conductance on the fractionation after carboxylation**

371 Mesophyll conductance, g_m , has been identified to coordinate with environmental factors more
372 rapidly than stomatal conductance (Galmés et al., 2007; Tazoe et al., 2011; Flexas et al., 2007). During
373 our 7-day cultivations, g_m increased and WUE_{ge} decreased with increasing SWC. It has been
374 documented that g_m can improve WUE under drought pretreatment (Han et al., 2016). However, the
375 mechanism by which g_m responds to the fluctuation of $[\text{CO}_2]$ is unclear. Terashima *et al.* (2006)
376 demonstrated that CO_2 permeable aquaporin, located in the plasma membrane and inner envelope of
377 chloroplasts, could regulate the change in g_m . In our study, g_m is species-specific to the $[\text{CO}_2]$ gradient.
378 The g_m in *P. orientalis* significantly decreased by **9.1-44.4%** from C_{600} to C_{800} at 60-80% of FC; these
379 are similar to the results of Flexas *et al.* (2007). A larger g_m in *Q. variabilis* under C_{800} was observed
380 compared to *P. orientalis*.

381 Furthermore, g_m contributed to the total ^{13}C fractionation that followed carboxylation, while
382 photosynthate had not been transported to the sapling twigs. The ^{13}C fractionation of CO_2 from the air
383 surrounding the leaf to sub-stomatal cavities may be simply explained by stomatal resistance, which
384 also contains the fractionation derived from mesophyll conductance between sub-stomatic cavities and
385 the site of carboxylation in the chloroplast that cannot be neglected and should be elucidated (Pons et
386 al., 2009; Cano et al., 2014). In estimating the post-carboxylation fractionation, g_m -sourced
387 fractionation must be subtracted from the total ^{13}C fractionation (the difference between $\delta^{13}\text{C}_{\text{WSC}}$ and
388 $\delta^{13}\text{C}_{\text{model}}$), which is closely associated with g_m (Fig. 8, $p=0.01$). Variations in g_m -sourced fractionation
389 are coordinated with those in g_m with changing environmental conditions (Table 2).

390 **4.4 Post-carboxylation fractionation generated before photosynthate moves out of leaves**

391 Photosynthesis, a biochemical and physiological process (Badeck et al., 2005), is characterized by
392 discrimination in ^{13}C , which leaves an isotopic signature in the photosynthetic apparatus. Farquhar *et al.*
393 (1989) reviewed the carbon-fractionation in leaves and covered the significant aspects of
394 photosynthetic carbon isotope discrimination. The post-carboxylation/photosynthetic fractionation
395 associated with the metabolic pathways of non-structural carbohydrates (NSC; defined here as soluble
396 sugars + starch) within leaves, and fractionation during translocation, storage, and remobilization prior
397 to tree ring formation is unclear (Epron et al., 2012; Gessler et al., 2014; Rinne et al., 2016). The
398 synthesis of sucrose and starch before transportation to twigs falls within the domain of
399 post-carboxylation fractionation generated in leaves. Hence, we hypothesized that ^{13}C fractionation

400 may exist. When we completed the leaf gas-exchange measurements, leaf samples were collected
401 immediately to determine the $\delta^{13}\text{C}_{WSC}$. Presumably, ^{13}C fractionation generated in the synthetic
402 processes of sucrose and starch was contained within the ^{13}C fractionation from the site of
403 carboxylation to cytoplasm before sugar transportation. Comparing $\delta^{13}\text{C}_{WSC}$ with $\delta^{13}\text{C}_{obs}$, the total ^{13}C
404 fractionation in *P. orientalis* ranged from 0.0328 to 0.0472‰, which was somewhat less than that in *Q.*
405 *variabilis* (from 0.0384 to 0.0466‰). Post-carboxylation fractionation contributed 75.3-98.9% to total
406 ^{13}C fractionation, determined by subtracting the fractionation in g_m from total ^{13}C fractionation. Gessler
407 et al. (2004) reviewed the environmental components of variation in photosynthetic carbon isotope
408 discrimination in terrestrial plants. Total ^{13}C fractionation in *P. orientalis* was enhanced by the increase
409 in SWC, consistent with that in *Q. variabilis*, except at 100% of FC. The ^{13}C isotope signature in *P.*
410 *orientalis* was depleted with elevated $[\text{CO}_2]$. Yet, ^{13}C -depletion was weakened in *Q. variabilis* for C_{600}
411 and C_{800} . Linear regressions between g_s and total ^{13}C fractionation indicated that the post-carboxylation
412 fractionation in leaves depends on the variation of g_s and that stomata aperture was correlated with
413 environmental change.

414 5 Conclusions

415 Through orthogonal treatments of four $[\text{CO}_2]$ \times five SWC, WUE_{cp} calculated by $\delta^{13}\text{C}_{WSC}$ and WUE_{ge}
416 derived from simultaneous leaf gas-exchange, were estimated to differentiate the $\delta^{13}\text{C}$ signal variation
417 before leaf-level translocation of primary assimilates. The influence of g_m on ^{13}C fractionation between
418 the sites of carboxylation and ambient air is important. It requires consideration when testing the
419 hypothesis that the post-carboxylation contributes to the ^{13}C fractionation from the site of carboxylation
420 to cytoplasm before sugar transport. In response to the interactive effects of $[\text{CO}_2]$ and SWC, WUE_{ge} in
421 the two tree species both decreased with increasing SWC, and increased with elevated $[\text{CO}_2]$ at 35–80%
422 of FC. We concluded that relative soil drying, coupled with elevated $[\text{CO}_2]$, can improve WUE_{ge} by
423 strengthening photosynthetic capacity and reducing transpiration. WUE_{ge} in *P. orientalis* was
424 significantly greater than that in *Q. variabilis*, while the opposite was the case for WUE_{cp} . The g_m and
425 post-carboxylation both contributed to the total ^{13}C fractionation. Rising $[\text{CO}_2]$ and/or moistening soil
426 generated increasing disparities between $\delta^{13}\text{C}_{WSC}$ and $\delta^{13}\text{C}_{model}$ in *P. orientalis*; nevertheless, the
427 differences between $\delta^{13}\text{C}_{WSC}$ and $\delta^{13}\text{C}_{model}$ in *Q. variabilis* increased when $[\text{CO}_2]$ was less than 600 ppm
428 and/or water stress was alleviated. Total ^{13}C fractionation in the leaf was linearly dependent on g_s . With
429 respect to carbon isotope fractionation in post-carboxylation and transportation processes, we note that
430 ^{13}C fractionation derived from the synthesis of sucrose and starch is likely influenced by environmental
431 changes. A clear description of the magnitude and environmental dependence of post-carboxylation
432 fractionation is worth considering.

433 References

- 434 Adiredjo, A. L., Navaud, O., Lamaze, T., and Grieu, P.: Leaf carbon isotope discrimination as an
435 accurate indicator of water use efficiency in sunflower genotypes subjected to five stable soil
436 water contents, *J Agron. Crop Sci.*, 200, 416–424, 2014.
- 437 Ainsworth, E. A. and McGrath, J. M.: Direct effects of rising atmospheric carbon dioxide and ozone on
438 crop yields, *Climate Change and Food Security*, Springer, 109–130, 2010.
- 439 Badeck, F. W., Tcherkez, G., Eacute, N. S. S., Piel, C. E. M., and Ghashghaie, J.: Post-photosynthetic
440 fractionation of stable carbon isotopes between plant organ – a widespread phenomenon, *Rapid*

441 Commun. Mass S., 19, 1381–1391, 2005.

442 Bögelein, R., Hassdenteufel, M., Thomas, F. M., and Werner, W.: Comparison of leaf gas exchange
443 and stable isotope signature of water-soluble compounds along canopy gradients of co-occurring
444 Douglas-fir and European beech, *Plant Cell Environ.*, 35, 1245–1257, 2012.

445 Brandes, E., Kodama, N., Whittaker, K., Weston, C., Rennenberg, H., Keitel, C., Adams, M. A., and
446 Gessler, A.: Short-term variation in the isotopic composition of organic matter allocated from the
447 leaves to the stem of *Pinus sylvestris*: effects of photosynthetic and postphotosynthetic carbon
448 isotope fractionation, *Global Change Biol.*, 12, 1922–1939, 2006.

449 Brooks, A. and Farquhar, G. D.: Effect of temperature on the CO₂/O₂ specificity of
450 ribulose-1,5-bisphosphate carboxylase/oxygenase and the rate of respiration in the light, *Planta*,
451 165, 397–406, 1985.

452 Brugnoli E, Farquhar GD. 2000. Photosynthetic fractionation of carbon isotopes. In: Leegood RC,
453 Sharkey TD, von Caemmerer S. eds. Photosynthesis: physiology and metabolism. Advances in
454 photosynthesis. Dordrecht, The Netherlands: Kluwer Academic Publishers, 399–434.

455 Cano, F. J., López, R., and Warren, C. R.: Implications of the mesophyll conductance to CO₂ for
456 photosynthesis and water-use efficiency during long-term water stress and recovery in two
457 contrasting Eucalyptus species, *Plant Cell Environ.*, 37, 2470–2490, 2014.

458 Cernusak, L. A., Ubierna, N., Winter, K., Holtum, J. A. M., Marshall, J. D., and Farquhar, G. D.:
459 Environmental and physiological determinants of carbon isotope discrimination in terrestrial
460 plants, *New Phytologist*, 200, 950–965, 2013.

461 DeLucia, E. H. and Heckathorn, S. A.: The effect of soil drought on water-use efficiency in a
462 contrasting Great Basin desert and Sierran montane species, *Plant Cell Environ.*, 12, 935–940,
463 1989.

464 Epron, D., Nouvellon, Y., and Ryan, M. G.: Introduction to the invited issue on carbon allocation of
465 trees and forests, *Tree physiol.*, 32, 639–643, 2012.

466 Evans, J. R., Kaldenhoff, R., Genty, B., and Terashima, I.: Resistances along the CO₂ diffusion
467 pathway inside leaves, *J. Exp. Bot.*, 60, 2235–2248, 2009.

468 Evans, J. R., Sharkey, T. D., Berry, J. A., and Farquhar, G. D.: Carbon isotope discrimination measured
469 concurrently with gas-exchange to investigate CO₂ diffusion in leaves of higher-plants, *Funct.*
470 *Plant Biol.*, 13, 281–292, 1986.

471 Evans, J. R. and von Caemmerer, S.: Temperature response of carbon isotope discrimination and
472 mesophyll conductance in tobacco, *Plant Cell Environ.*, 36, 745–756, 2013.

473 Farquhar, G. D., Ehleringer, J. R., and Hubick, K. T.: Carbon isotope discrimination and
474 photosynthesis, *Ann. Rev. Plant Physiol.*, 40, 503–537, 1989.

475 Farquhar, G. D., O'Leary, M. H., and Berry, J. A.: On the relationship between carbon isotope
476 discrimination and the intercellular carbon dioxide concentration in leaves, *Funct. Plant Biol.*, 9,
477 121–137, 1982.

478 Farquhar, G. D. and Sharkey, T. D.: Stomatal conductance and photosynthesis, *Ann. Rev. Plant*
479 *Physiol.*, 33, 317–345, 1982.

480 Flexas, J., Barbour, M. M., Brendel, O., Cabrera, H. M., Carriqui J M., D áz-Espejo, A., Douthe, C.,
481 Dreyer, E., Ferrio, J. P., Gago, J., Gallé A., Galmés, J., Kodama, N., Medrano, H., Niinemets, Ü.,
482 Peguero-Pina, J. J., Pou, A., Ribas-Carbó, M., Tomás, M., Tosens, T., and Warren, C. R.:
483 Mesophyll diffusion conductance to CO₂: An unappreciated central player in photosynthesis, *Plant*
484 *Science*, 193–194, 70–84, 2012.

485 Flexas, J., Carriquí M., Coopman, R. E., Gago, J., Galmés, J., Martorell, S., Morales, F., and
486 Diaz-Espejo, A.: Stomatal and mesophyll conductances to CO₂ in different plant groups:
487 Underrated factors for predicting leaf photosynthesis responses to climate change? *Plant Science*,
488 226, 41–48, 2014.

489 Flexas, J., Diaz-Espejo, A., Galmés, J., Kaldenhoff, R., Medano, H., and Ribas-Carbo, M.: Rapid
490 variations of mesophyll conductance in response to changes in CO₂ concentration around leaves,
491 *Plant Cell Environ.*, 30, 1284–1298, 2007.

492 Flexas, J., Ribas-Carbó, M., Diaz-Espejo, A., Galmés, J., and Medrano, H.: Mesophyll conductance to
493 CO₂: current knowledge and future prospects, *Plant Cell Environ.*, 31, 602–621, 2008.

494 Flexas, J., Ribas-Carbó, M., Hanson, D.T., Bota, J., Otto, B., Cifre, J., McDowell, N., Medrano, H., and
495 Kaldenhoff, R.: Tobacco aquaporin NtAQP1 is involved in mesophyll conductance to CO₂ *in vivo*,
496 *Plant J.*, 48, 427–439, 2006.

497 Galmés, J., Medrano, H., and Flexas, J.: Photosynthetic limitations in response to water stress and
498 recovery in Mediterranean plants with different growth forms, *New Phytol.*, 175, 81–93, 2007.

499 Gessler, A., Brandes, E., Buchmann, N., Helle, G., Rennenberg, H., and Barnard, R. L.: Tracing carbon
500 and oxygen isotope signals from newly assimilated sugars in the leaves to the tree-ring archive,
501 *Plant Cell Environ.*, 32, 780–795, 2009.

502 Gessler, A., Ferrio, J. P., Hommel, R., Treydte, K., Werner, R. A., and Monson, R. K.: Stable isotopes
503 in tree rings: towards a mechanistic understanding of isotope fractionation and mixing processes
504 from the leaves to the wood, *Tree Physiol.*, 34, 796–818, 2014.

505 Gessler, A., Rennenberg, H., and Keitel, C.: Stable isotope composition of organic compounds
506 transported in the phloem of European beech-evaluation of different methods of phloem sap
507 collection and assessment of gradients in carbon isotope composition during leaf-to-stem transport,
508 *Plant Biology*, 6, 721–729, 2004.

509 Gessler, A., Tcherkez, G., Peuke, A. D., Ghashghaie, J., and Farquhar, G. D.: Experimental evidence
510 for diel variations of the carbon isotope composition in leaf, stem and phloem sap organic matter
511 in *Ricinus communis*, *Plant Cell Environ.*, 31, 941–953, 2008.

512 Gillon, J. S., Griffiths, H.: The influence of (photo)respiration on carbon isotope discrimination in
513 plants. *Plant Cell Environ.*, 20, 1217–1230, 1997.

514 Gleixner, G. and Schmidt, H.: Carbon isotope effects on the fructose-1, 6-bisphosphate aldolase
515 reaction, origin for non-statistical ¹³C distributions in carbohydrates, *J. Biol. Chem.*, 272, 5382–
516 5387, 1997.

517 Guy, R. D., Fogel, M. L., and Berry, J. A.: Photosynthetic fractionation of the stable isotopes of oxygen
518 and carbon, *Plant Physiol.*, 101, 37–47, 1993.

519 Han, J. M., Meng, H. F., Wang, S. Y., Jiang, C. D., Liu, F., Zhang, W. F., and Zhang, Y. L.: Variability
520 of mesophyll conductance and its relationship with water use efficiency in cotton leaves under
521 drought pretreatment, *J. Plant Physiol.*, 194, 61–71, 2016.

522 Hommel, R., Siegwolf, R., Saurer, M., Farquhar, G. D., Kayler, Z., Ferrio, J. P., and Gessler, A.:
523 Drought response of mesophyll conductance in forest understory species-impacts on water-use
524 efficiency and interactions with leaf water movement, *Physiol. Plantarum*, 152, 98–114, 2014.

525 Igamberdiev, A. U., Mikkelsen, T. N., Ambus, P., Bauwe, H., and Lea, P. J.: Photorespiration
526 contributes to stomatal regulation and carbon isotope fractionation: a study with barley, potato and
527 Arabidopsis plants deficient in glycine decarboxylase, *Photosynth. Res.*, 81, 139–152, 2004.

528 IPCC: Summary for policymakers, in: *Climate Change 2014, Mitigation of Climate Change*,

529 contribution of Working Group III to the Fifth Assessment Report of the Intergovernmental Panel
530 on Climate Change, edited by: Edenhofer, O., Pichs-Madruga, R., Sokona, Y., Farahani, E.,
531 Kadner, S., Seyboth, K., Adler, A., Baum, I., Brunner, S., Eickemeier, P., Kriemann, B.,
532 Savolainen, J., Schlomer, S., von Stechow, C., Zwickel, T., and Minx, J. C., Cambridge
533 University Press, Cambridge, UK and New York, NY, USA, 1–30, 2014.

534 Jäggi, M., Saurer, M., Fuhrer, J., and Siegwolf, R.: The relationship between the stable carbon isotope
535 composition of needle bulk material, starch, and tree rings in *Picea abies*, *Oecologia*, 131, 325–
536 332, 2002.

537 Kadam, N. N., Xiao, G., Melgar, R. J., Bahuguna, R. N., Quinones, C., Tamilselvan, A., Prasad, P. V.
538 V., and Jagadish, K. S. V.: Chapter three-agronomic and physiological responses to high
539 temperature, drought, and elevated CO₂ interactions in cereals, *Adv. Agron.*, 127, 111–156, 2014.

540 Kgope, B. S., Bond, W. J., and Midgley, G. F.: Growth responses of African savanna trees implicate
541 atmospheric [CO₂] as a driver of past and current changes in savanna tree cover, *Austral Ecol.*, 35,
542 451–463, 2010.

543 Kirkham, M. B.: Elevated carbon dioxide: impacts on soil and plant water relations, CRC Press,
544 London, New York, 2016.

545 Kodama, N., Barnard, R. L., Salmon, Y., Weston, C., Ferrio, J. P., Holst, J., Werner, R. A., Saurer, M.,
546 Rennenberg, H., and Buchmann, N.: Temporal dynamics of the carbon isotope composition in a
547 *Pinus sylvestris* stand: from newly assimilated organic carbon to respired carbon dioxide,
548 *Oecologia*, 156, 737–750, 2008.

549 Lanigan, G. J., Betson, N., Griffiths, H., and Seibt, U.: Carbon isotope fractionation during
550 photorespiration and carboxylation in *Senecio*, *Plant Physiol.*, 148, 2013–2020, 2008.

551 Le Roux, X., Bariac, T., Sinoquet H., Genty, B., Piel, C., Mariotti, A., Girardin, C., and Richard, P.:
552 Spatial distribution of leaf water-use efficiency and carbon isotope discrimination within an
553 isolated tree crown, *Plant Cell Environ.*, 24, 1021–1032, 2001.

554 Leakey, A. D.: Rising atmospheric carbon dioxide concentration and the future of C4 crops for food
555 and fuel, *Proceedings of the Royal Society of London B: Biological Sciences*, 276, 1517–2008,
556 2009.

557 Leakey, A. D., Ainsworth, E. A., Bernacchi, C. J., Rogers, A., Long, S. P., and Ort, D. R.: Elevated
558 CO₂ effects on plant carbon, nitrogen, and water relations: six important lessons from FACE, *J.*
559 *Exp. Bot.*, 60, 2859–2876, 2009.

560 Lobell, D. B., Roberts, M. J., Schlenker, W., Braun, N., Little, B. B., Rejesus, R. M., and Hammer, G.
561 L.: Greater sensitivity to drought accompanies maize yield increase in the US Midwest, *Science*,
562 344, 516–519, 2014.

563 Medlyn, B. E., Barton, C. V. M., Broadmeadow, M. S. J., Ceulemans, R., Angelis, P. D., Forstreuter,
564 M., Freeman, M., Jackson, S. B., Kellomäki, S., and Laitat, E.: Stomatal conductance of forest
565 species after long-term exposure to elevated CO₂ concentration: a synthesis, *New Phytol.*, 149,
566 247–264, 2001.

567 Mielke, M. S., Oliva, M. A., de Barros, N. F., Penchel, R. M., Martinez, C. A., Da Fonseca, S., and de
568 Almeida, A. C.: Leaf gas exchange in a clonal eucalypt plantation as related to soil moisture, leaf
569 water potential and microclimate variables, *Trees*, 14, 263–270, 2000.

570 Micanda Apodaca, J., Pérez López, U., Lacuesta, M., Mena Petite, A., and Muñoz Rueda, A.: The type
571 of competition modulates the ecophysiological response of grassland species to elevated CO₂ and
572 drought, *Plant Biolog.*, 17, 298–310, 2014.

573 Parker, W. C. and Pallardy, S. G.: Gas exchange during a soil drying cycle in seedlings of four black
574 walnut (*Juglans nigra* L.) Families, *Tree physiol.*, 9, 339–348, 1991.

575 Pons, T. L., Flexas, J., von Caemmerer, S., Evans, J. R., Genty, B., Ribas-Carbo, M., and Brugnoli, E.:
576 Estimating mesophyll conductance to CO₂: methodology, potential errors, and recommendations,
577 *J. Exp. Bot.*, 8, 1–18, 2009.

578 Reich, P. B., Walters, M. B., and Tabone, T. J.: Response of *Ulmus americana* seedlings to varying
579 nitrogen and water status. 2 Water and nitrogen use efficiency in photosynthesis, *Tree Physiol.*, 5,
580 173–184, 1989.

581 Rinne, K. T., Saurer, M., Kirdeyanov, A. V., Bryukhanova, M. V., Prokushkin, A. S., Churakova
582 Sidorova, O. V., and Siegwolf, R. T.: Examining the response of larch needle carbohydrates to
583 climate using compound-specific δ¹³C and concentration analyses, EGU General Assembly
584 Conference, 1814949R, 2016.

585 Robredo, A., Pérez-López, U., de la Maza, H. S., González-Moro, B., Lacuesta, M., Mena-Petite, A.,
586 and Muñoz-Rueda, A.: Elevated CO₂ alleviates the impact of drought on barley improving water
587 status by lowering stomatal conductance and delaying its effects on photosynthesis, *Environ. Exp.*
588 *Bot.*, 59, 252–263, 2007.

589 Robredo, A., Pérez-López, U., Lacuesta, M., Mena-Petite, A., and Muñoz-Rueda, A.: Influence of
590 water stress on photosynthetic characteristics in barley plants under ambient and elevated CO₂
591 concentrations, *Biologia. Plantarum*, 54, 285–292, 2010.

592 Rossmann, A., Butzenlechner, M., and Schmidt, H.: Evidence for a nonstatistical carbon isotope
593 distribution in natural glucose, *Plant Physiol.*, 96, 609–614, 1991.

594 Streit, K., Rinne, K. T., Hagedorn, F., Dawes, M. A., Saurer, M., Hoch, G., Werner, R. A., Buchmann,
595 N., and Siegwolf, R. T. W.: Tracing fresh assimilates through *Larix decidua* exposed to elevated
596 CO₂ and soil warming at the alpine treeline using compound-specific stable isotope analysis, *New*
597 *Phytol.*, 197, 838–849, 2013.

598 Tausz Posch, S., Norton, R. M., Seneweera, S., Fitzgerald, G. J., and Tausz, M.: Will intra-specific
599 differences in transpiration efficiency in wheat be maintained in a high CO₂ world? A FACE study,
600 *Physiol. Plantarum*, 148, 232–245, 2013.

601 Tazoe, Y., von Caemmerer, S., Estavillo, G. M., and Evans, J. R.: Using tunable diode laser
602 spectroscopy to measure carbon isotope discrimination and mesophyll conductance to CO₂
603 diffusion dynamically at different CO₂ concentrations, *Plant Cell Environ.*, 34, 580–591, 2011.

604 Terashima, I., Hanba, Y.T., Tazoe, Y., Vyas, P., and Yano, S.: Irradiance and phenotype: comparative
605 eco-development of sun and shade leaves in relation to photosynthetic CO₂ diffusion, *J. Exp. Bot.*,
606 57, 343–354, 2006.

607 Théroux-Rancourt, G., Éhier, G., and Pepin, S.: Threshold response of mesophyll CO₂ conductance to
608 leaf hydraulics in highly transpiring hybrid poplar clones exposed to soil drying, *J. Exp. Bot.*, 65,
609 741–753, 2014.

610 Von Caemmerer, S. V. and Farquhar, G. D.: Some relationships between the biochemistry of
611 photosynthesis and the gas exchange of leaves, *Planta*, 153, 376–387, 1981.

612 Wall, G. W., Garcia, R. L., Kimball, B. A., Hunsaker, D. J., Pinter, P. J., Long, S. P., Osborne, C. P.,
613 Hendrix, D. L., Wechsung, F., and Wechsung, G.: Interactive effects of elevated carbon dioxide
614 and drought on wheat, *Agron. J.*, 98, 354–381, 2006.

615 Wall, G. W., Garcia, R. L., Wechsung, F., and Kimball, B. A.: Elevated atmospheric CO₂ and drought
616 effects on leaf gas exchange properties of barley, *Agr. Ecosyst. Environ.*, 144, 390–404, 2011.

617 Warren, C. R. and Adams, M. A.: Internal conductance does not scale with photosynthetic capacity:
618 implications for carbon isotope discrimination and the economics of water and nitrogen use in
619 photosynthesis, *Plant Cell Environ.*, 29, 192–201, 2006.
620 Xu, D. Q.: Some problems in stomatal limitation analysis of photosynthesis, *Plant Physiol. J.*, 33, 241–
621 244, 1997.
622 Xu, Z. and Zhou, G.: Responses of photosynthetic capacity to soil moisture gradient in perennial
623 rhizome grass and perennial bunchgrass, *BMC Plant Boil.*, 11, 21, 2011.
624 Yang, B., Pallardy, S. G., Meyers, T. P., GU, L. H., Hanson, P. J., Wullschleger, S. D., Heuer, M.,
625 Hosman, K. P., Riggs, J. S., and Sluss D. W.: Environmental controls on water use efficiency
626 during severe drought in an Ozark Forest in Missouri, USA, *Global Change Biol.*, 16, 2252–2271,
627 2010.
628 Yu, G., Wang, Q., and Mi, N.: *Ecophysiology of plant photosynthesis, transpiration, and water use*,
629 Science Press, Beijing, China, 2010.
630

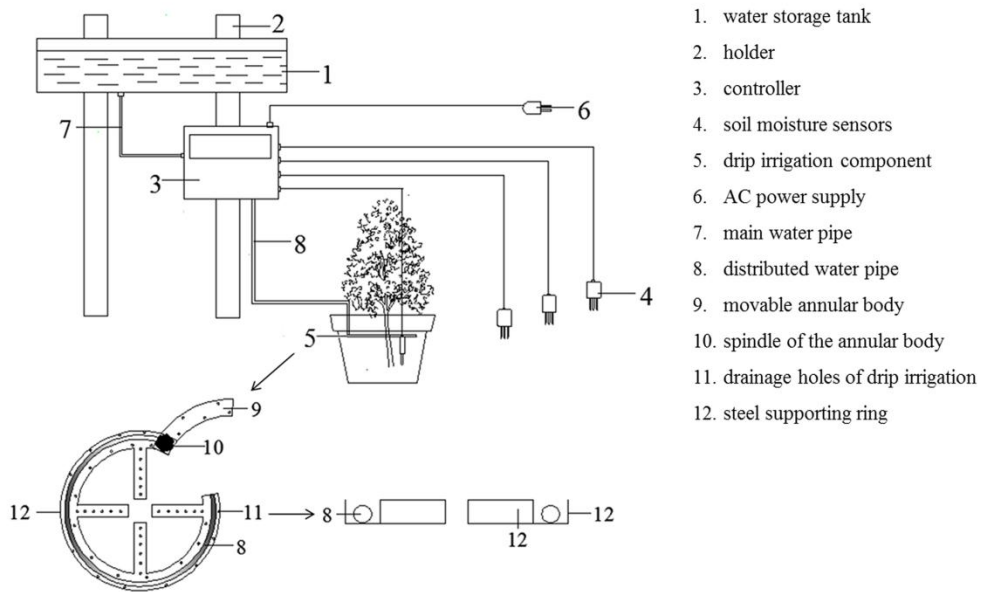
631 **Author contributions**

632 N. Zhao and Y. He collected field samples, and performed the experiments. N. Zhao analyzed the data
633 and wrote the paper. P. Meng commented on the theory and study design. X. Yu revised and edited the
634 manuscript.

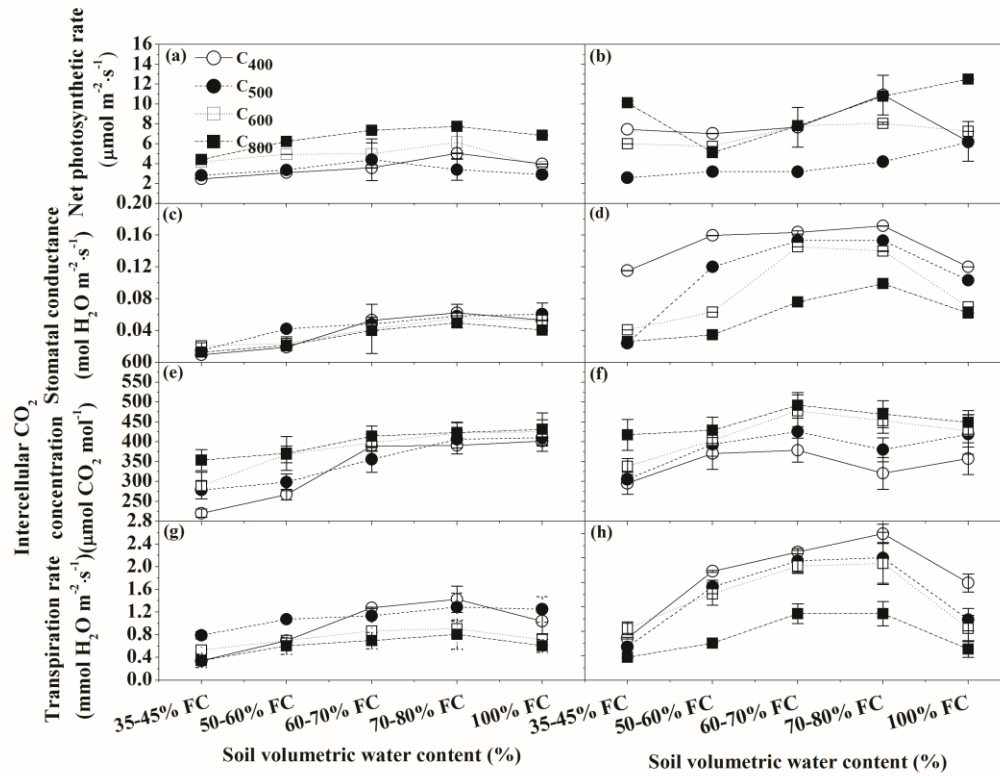
635

636 *Acknowledgements.* Financial support for this project was provided by the National Natural Science
637 Foundation of China (grant No. 41430747) and the Beijing Municipal Education Commission
638 (CEFF-PXM2017_014207_000043). We thank Beibei Zhou and Yuanhai Lou for collection of
639 materials and management of saplings. We are grateful to anonymous reviewers for constructive
640 suggestions regarding this manuscript. Due to space limitations we cited selected references involving
641 this study topic and apologize for authors whose work was not cited.

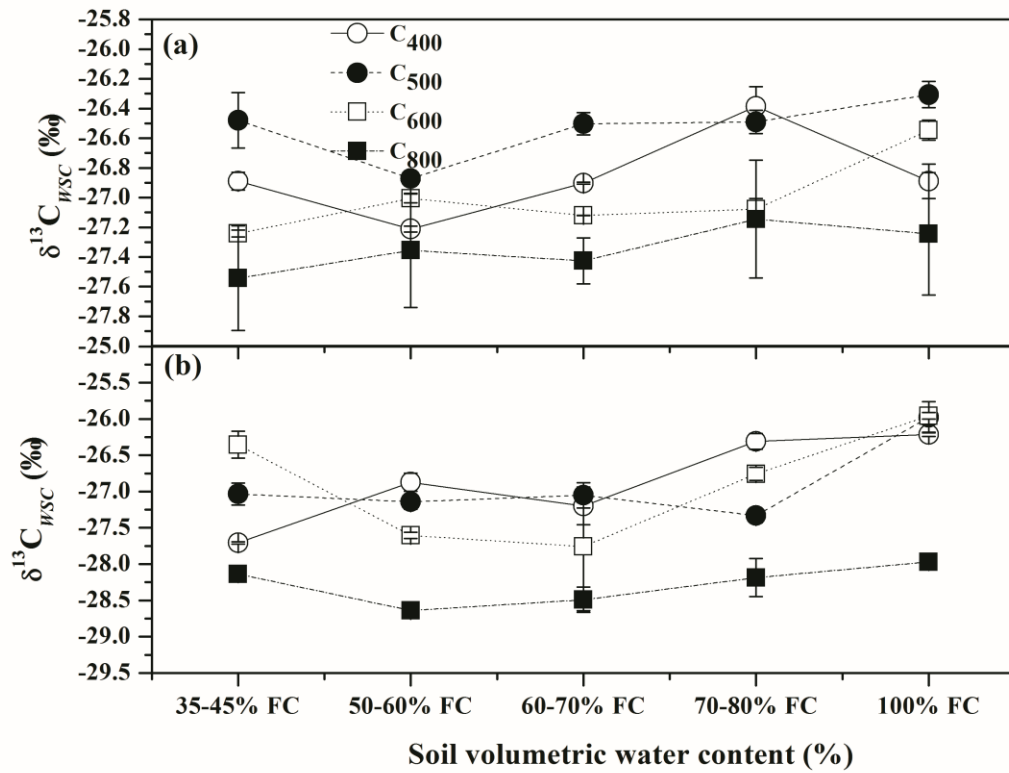
Figure



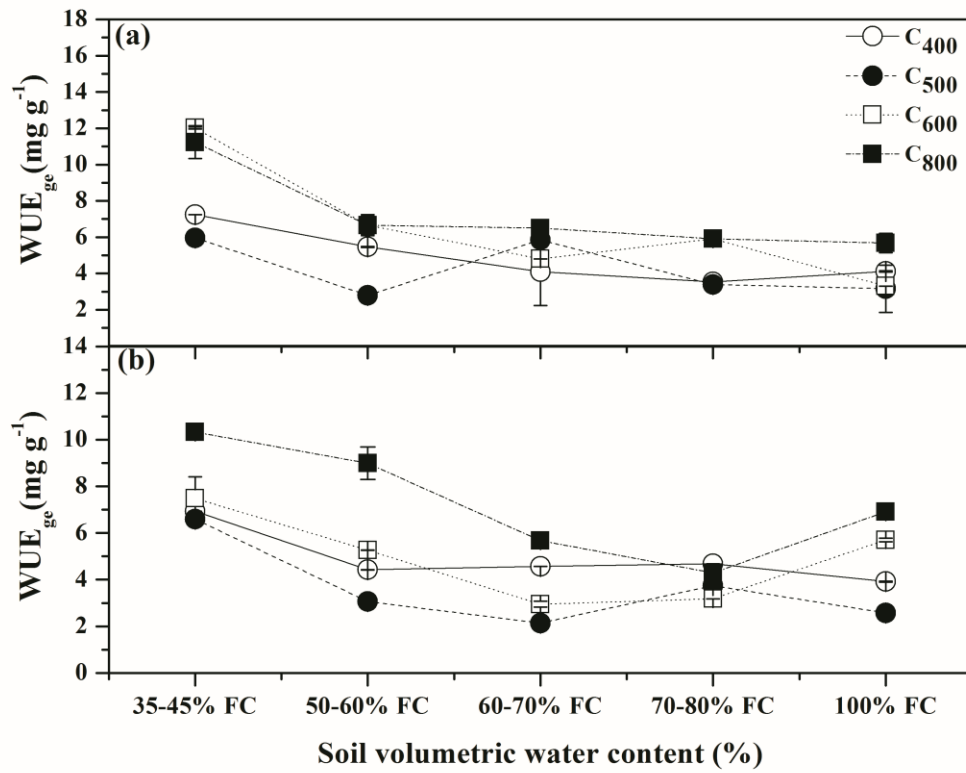
643 **Figure 1.** Diagram of the automatic drip irrigation device used in this study; numbers indicate the
 644 individual parts of the irrigation device (No. 1–12). The lower-left corner of this figure presents the
 645 detailed schematic for the drip irrigation component (No. 8–12).



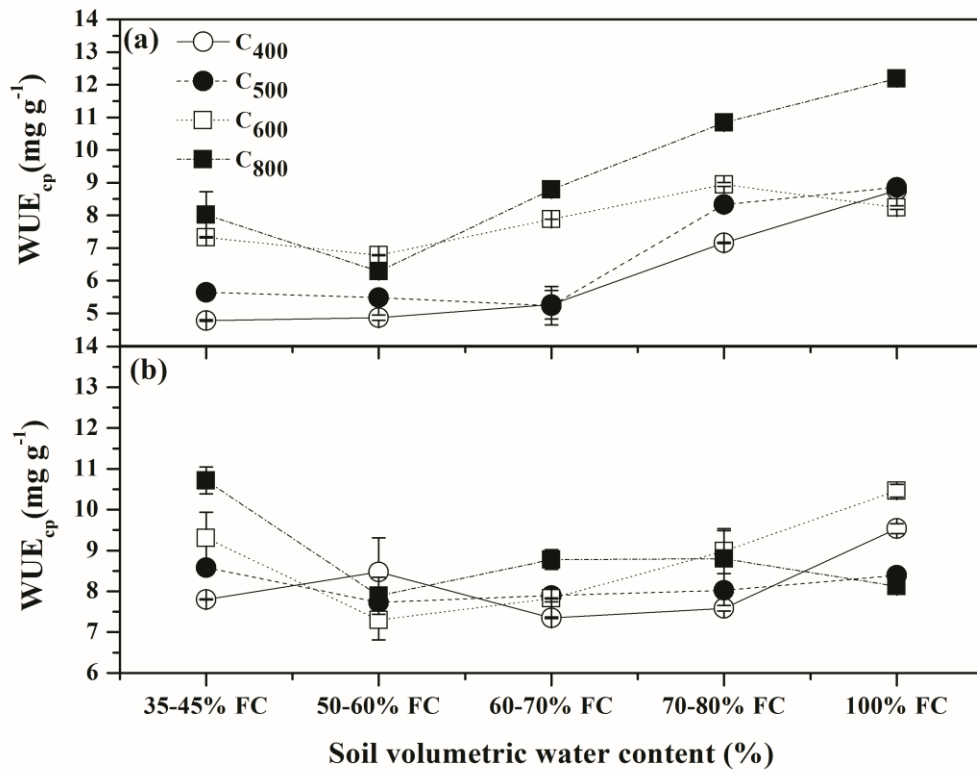
646 **Figure 2.** Net photosynthetic rates (P_n , $\mu\text{mol m}^{-2} \text{s}^{-1}$, a and b), stomatal conductance (g_s , $\text{mol H}_2\text{O m}^{-2}$
647 s^{-1} , c and d), intercellular CO_2 concentration (C_i , $\mu\text{mol CO}_2 \text{ mol}^{-1}$, e and f), and transpiration rates (T_r ,
648 $\text{mmol H}_2\text{O m}^{-2} \text{s}^{-1}$, g and h) in *P. orientalis* and *Q. variabilis* for four CO_2 concentration \times five soil
649 volumetric water content treatments. Means \pm SDs, $n = 32$.



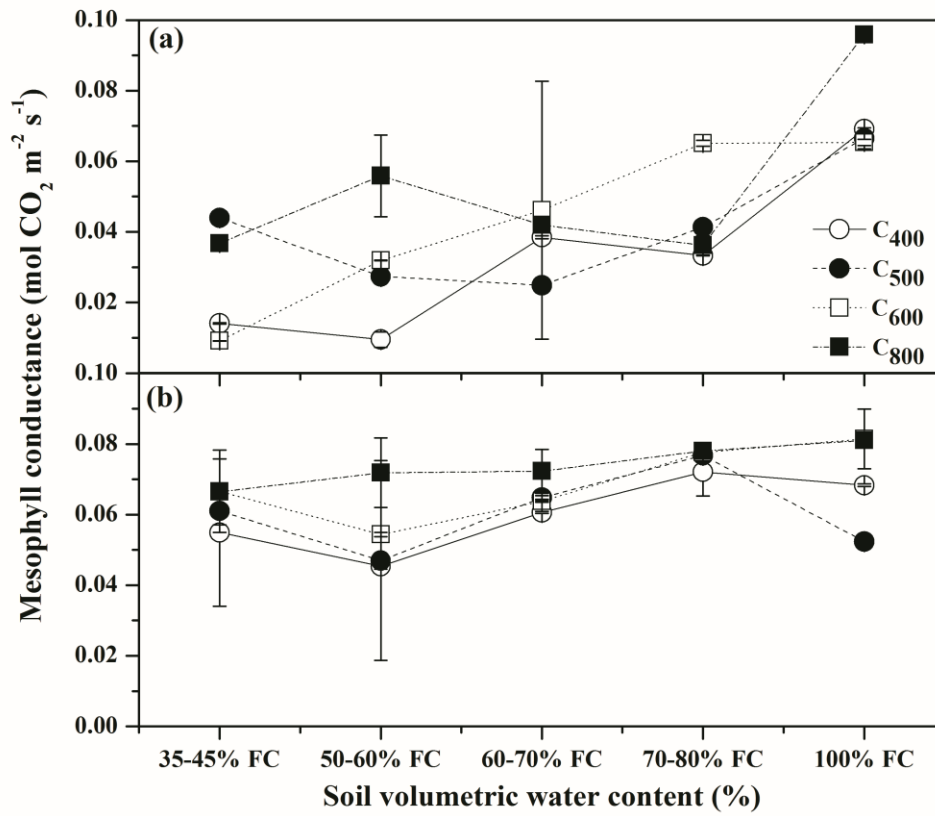
650 **Figure 3.** Carbon isotope composition of water-soluble compounds ($\delta^{13}\text{C}_{\text{WSC}}$) extracted from leaves of
 651 *P. orientalis* (a) and *Q. variabilis* (b) for four CO_2 concentration \times five soil volumetric water content
 652 treatments. Means \pm SDs, n=32.



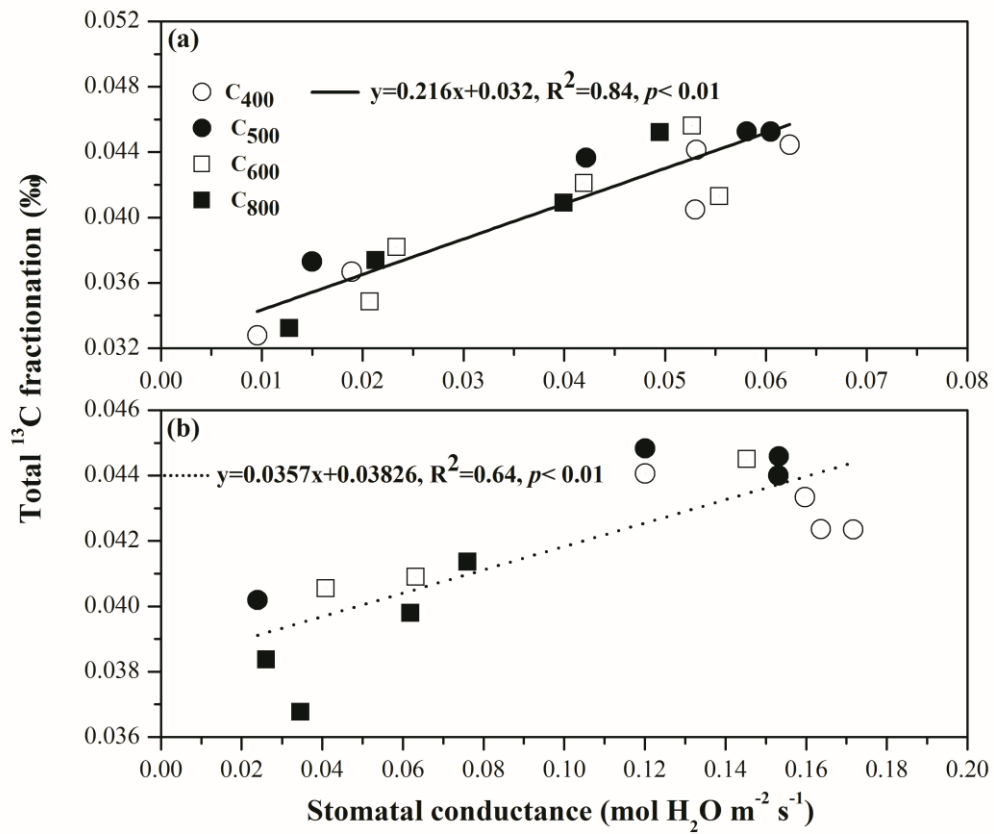
653 **Figure 4.** Instantaneous water use efficiency through gas exchange measurements (WUE_{ge}) for leaves
 654 from *P. orientalis* (a) and *Q. variabilis* (b) for four CO₂ concentration × five soil volumetric water
 655 content treatments. Means ±SDs, n= 32.



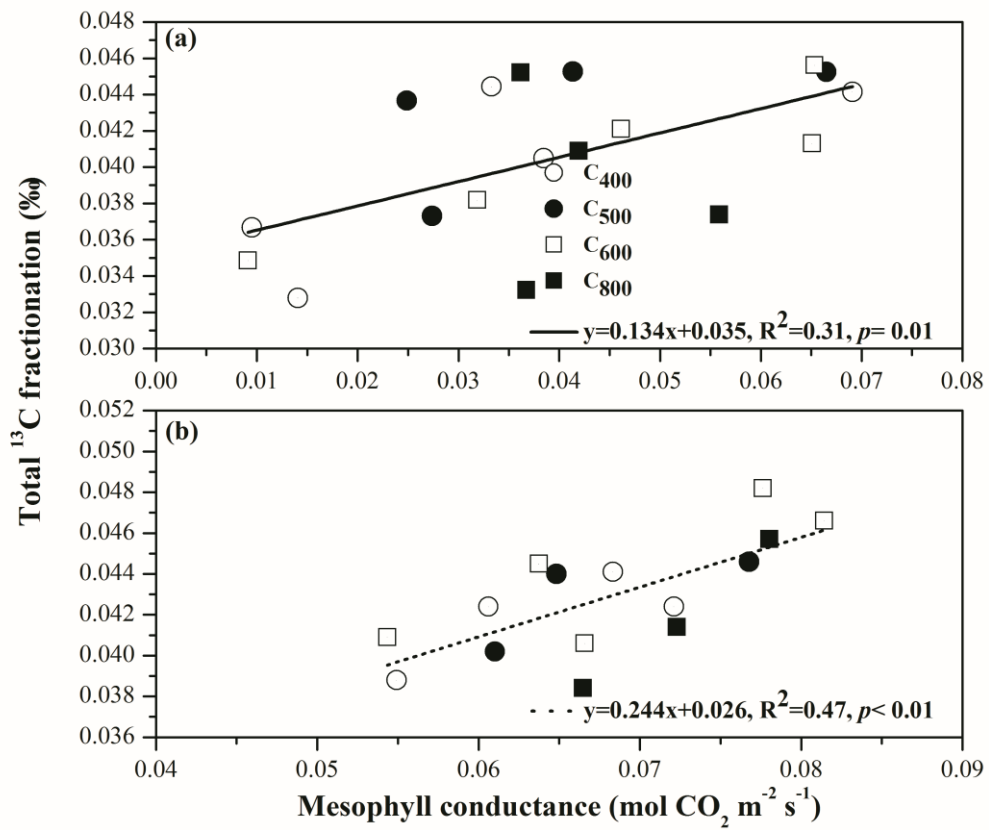
656 **Figure 5.** Instantaneous water use efficiency estimated by $\delta^{13}\text{C}$ of water-soluble compounds (WUE_{cp})
 657 from leaves of *P. orientalis* (a) and *Q. variabilis* (b) for four CO₂ concentration × five soil volumetric
 658 water content treatments. Means ±SDs, n= 32.



659 **Figure 6.** Mesophyll conductance in *P. orientalis* (a) and *Q. variabilis* (b) for four CO₂ concentration ×
 660 five soil volumetric water content treatments. Means ±SDs, n= 32.



661 **Figure 7.** Regressions between stomatal conductance and total ^{13}C fractionation in *P. orientalis* (a) and
 662 *Q. variabilis* (b) for four CO_2 concentration \times five soil volumetric water content treatments ($p<0.01$,
 663 $n=32$).



664 **Figure 8.** Regressions between mesophyll conductance and total ^{13}C fractionation in *P. orientalis* (a)
 665 and *Q. variabilis* (b) for four CO₂ concentration \times five soil volumetric water content treatments ($p \leq$
 666 0.01, $n = 32$).

Table**Table 1.** Orthogonal treatments applied to *P. orientalis* and *Q. variabilis*.

<i>P. orientalis</i>	Repeats (cultivated period)	B ₁	B ₂	B ₃	B ₄	B ₅
A ₁	R ₁ :June 2–9	A ₁ B ₁ R ₁	A ₁ B ₂ R ₁	A ₁ B ₃ R ₁	A ₁ B ₄ R ₁	A ₁ B ₅ R ₁
	R ₂ :June 12–19	A ₁ B ₁ R ₂	A ₁ B ₂ R ₂	A ₁ B ₃ R ₂	A ₁ B ₄ R ₂	A ₁ B ₅ R ₂
A ₂	R ₁ :July 11–18	A ₂ B ₁ R ₁	A ₂ B ₂ R ₁	A ₂ B ₃ R ₁	A ₂ B ₄ R ₁	A ₂ B ₅ R ₁
	R ₂ :July 22–29	A ₂ B ₁ R ₂	A ₂ B ₂ R ₂	A ₂ B ₃ R ₂	A ₂ B ₄ R ₂	A ₂ B ₅ R ₂
A ₃	R ₁ :June 2–9	A ₃ B ₁ R ₁	A ₃ B ₂ R ₁	A ₃ B ₃ R ₁	A ₃ B ₄ R ₁	A ₃ B ₅ R ₁
	R ₂ :June 12–19	A ₃ B ₁ R ₂	A ₃ B ₂ R ₂	A ₃ B ₃ R ₂	A ₃ B ₄ R ₂	A ₃ B ₅ R ₂
A ₄	R ₁ :July 11–18	A ₄ B ₁ R ₁	A ₄ B ₂ R ₁	A ₄ B ₃ R ₁	A ₄ B ₄ R ₁	A ₄ B ₅ R ₁
	R ₂ :July 22–29	A ₄ B ₁ R ₂	A ₄ B ₂ R ₂	A ₄ B ₃ R ₂	A ₄ B ₄ R ₂	A ₄ B ₅ R ₂
<i>Q. variabilis</i>	Repeats (cultivated period)	B ₁	B ₂	B ₃	B ₄	B ₅
A ₁	P ₁ :June 21–28	A ₁ B ₁ P ₁	A ₁ B ₂ P ₁	A ₁ B ₃ P ₁	A ₁ B ₄ P ₁	A ₁ B ₅ P ₁
	P ₂ :July 2–9	A ₁ B ₁ P ₂	A ₁ B ₂ P ₂	A ₁ B ₃ P ₂	A ₁ B ₄ P ₂	A ₁ B ₅ P ₂
A ₂	P ₁ :August 4–11	A ₂ B ₁ P ₁	A ₂ B ₂ P ₁	A ₂ B ₃ P ₁	A ₂ B ₄ P ₁	A ₂ B ₅ P ₁
	P ₂ :August 15–22	A ₂ B ₁ P ₂	A ₂ B ₂ P ₂	A ₂ B ₃ P ₂	A ₂ B ₄ P ₂	A ₂ B ₅ P ₂
A ₃	P ₁ :June 21–28	A ₃ B ₁ P ₁	A ₃ B ₂ P ₁	A ₃ B ₃ P ₁	A ₃ B ₄ P ₁	A ₃ B ₅ P ₁
	P ₂ :July 2–9	A ₃ B ₁ P ₂	A ₃ B ₂ P ₂	A ₃ B ₃ P ₂	A ₃ B ₄ P ₂	A ₃ B ₅ P ₂
A ₄	P ₁ :August 4–11	A ₄ B ₁ P ₁	A ₄ B ₂ P ₁	A ₄ B ₃ P ₁	A ₄ B ₄ P ₁	A ₄ B ₅ P ₁
	P ₂ :August 15–22	A ₄ B ₁ P ₂	A ₄ B ₂ P ₂	A ₄ B ₃ P ₂	A ₄ B ₄ P ₂	A ₄ B ₅ P ₂

670 **Table 2.** Carbon-13 isotope fractionation in *P. orientalis* and *Q. variabilis* under four CO₂ concentration × five soil volumetric water content treatments.

Species	SWC (of FC)	CO ₂ concentration (ppm)													
		¹³ C				¹³ C				¹³ C					
		400	500	600	800	fractionation (‰)	400	500	600	800	fractionation (‰)	400	500	600	800
<i>P. orientalis</i>	35–45%	0.0328	0.0373	0.0349	0.0332		0.0081	0.0030	0.0034	0.0072		0.0247	0.0343	0.0315	0.0260
	50–60%	0.0367	0.0437	0.0382	0.0374		0.0018	0.0058	0.0094	0.0004		0.0349	0.0379	0.0288	0.0370
	60–70%	0.0405	0.0366	0.0421	0.0409		0.0018	0.0050	0.0026	0.0007		0.0387	0.0316	0.0395	0.0402
	70–80%	0.0444	0.0453	0.0413	0.0452		0.0044	0.0052	0.0103	0.0013		0.0400	0.0401	0.0310	0.0439
	100%	Total ¹³ C fractionation (‰)	0.0441	0.0453	0.0456	0.0472	Mesophyll conductance	0.0057	0.0040	0.0025	0.0039	Post- photosynthesis	0.0384	0.0413	0.0431
<i>Q. variabilis</i>	35–45%	0.0388	0.0402	0.0406	0.0384		0.0007	0.0025	0.0006	0.0091		0.0381	0.0377	0.0400	0.0293
	50–60%	0.0433	0.0448	0.0409	0.0368		0.0061	0.0084	0.0023	0.0018		0.0372	0.0364	0.0386	0.0350
	60–70%	0.0424	0.0440	0.0445	0.0414		0.0066	0.0086	0.0078	0.0041		0.0358	0.0354	0.0367	0.0373
	70–80%	0.0424	0.0446	0.0482	0.0457		0.0034	0.0016	0.0074	0.0028		0.0390	0.0430	0.0408	0.0429
	100%	0.0441	0.0466	0.0466	0.0398		0.0027	0.0076	0.0022	0.0125		0.0414	0.0390	0.0444	0.0273

671